The E3 ligase TRIM31 regulates hematopoietic stem cell homeostasis and MLL-AF9 leukemia

Kai Zhang,[1,*] Dingdong Liu,[1,*] Yafei Li,[1] Zhencan Shi,[2] Jun Guo,[2] Chengjiang Gao,[3] Hu Wang,[1] Zhenyu Ju[1] and Daojun Diao[1]

[1]Key Laboratory of Regenerative Medicine of Ministry of Education, Institute of Aging and Regenerative Medicine, Jinan University, Guangzhou; [2]Department of Cardiology, the First Affiliated Hospital of Jinan University, Guangzhou and [3]Department of Immunology and Key Laboratory of Infection, Immunity of Shandong Province, Shandong University School of Basic Medical Sciences, Jinan, China.

**KZ and DL contributed equally as first authors.*

Correspondence: D. Diao
diaodaojun@hotmail.com

Z. Ju
zhenyuju@163.com

Received: August 18, 2022.
Accepted: December 28, 2022.
Early view: January 12, 2023.

https://doi.org/10.3324/haematol.2022.281955

Abstract

Hematopoietic stem cells (HSC) are kept in a quiescent state to maintain their self-renewal capacity. Proper regulation of cyclin-dependent kinases (CDK) and cyclin proteins is critical for the maintenance of HSC homeostasis. Here, we found that the E3 ligase, TRIM31, regulates HSC homeostasis and leukemia through the accumulation of CDK8. *TRIM31* deficiency promotes hematopoietic stem and progenitor cell proliferation and long-term HSC exhaustion. Serial competitive transplantation assays showed that TRIM31-deficient HSC exhibit impaired reconstitution ability. TRIM31 loss led to a lower rate of survival of mice under conditions of stress (5-fluorouracil administration), which was correlated with a lower number of hematopoietic stem and progenitor cells. In a murine model of acute myeloid leukemia, the initiation of leukemia was significantly accelerated upon *TRIM31* deletion. Mechanistically, we found that ubiquitin-mediated degradation of CDK8 was impaired by *TRIM31* deletion, which further induced transcriptional expression of *PBX1* and *cyclin D1*. Taken together, these findings reveal the function of TRIM31 in the regulation of HSC homeostasis and leukemia initiation, and indicate the physiological importance of TRIM31 in the early stage of the development of leukemia.

Introduction

Under steady conditions, hematopoietic stem cells (HSC) are in a quiescent state to prevent exhaustion of the cells and to restrict the occurrence of replication-associated mutations.[1] An uncontrolled self-renewal program disrupts stem cell maintenance, and over-proliferation of stem cells often leads to HSC exhaustion and leukemia.[2] Quality control of the cell cycle is achieved through cell-intrinsic regulators, including transcription factors, signal transducers, cell-cycle inhibitors, surface receptors, and cell-extrinsic factors, such as the bone marrow niche and cytokines. Notably, cell-intrinsic regulators can be manipulated by the ubiquitin-proteasome degradation system at the protein level.

Ubiquitin E3 ligases play a critical role in the hematopoietic system. Loss of E3 ligases (including c-Cbl, Itch and SCFF^{bxw7}) may affect HSC quiescence and lead to stem cell expansion, myeloid proliferative disorders and acute myeloid leukemia (AML).[3-5] As E3 ligases, TRIM proteins are widely involved in various cell processes, such as cell proliferation, differentiation, development and apoptosis. Some of them, notably TRIM19 and TRIM33, are vital for the maintenance and function of HSC.[6,7] Other members of the TRIM family, such as TRIM13 and TRIM24, have also been reported to be essential in various hematologic malignancies.[8,9] TRIM31, another TRIM family protein, is crucial for intracellular signaling, innate immunity, autophagy and carcinogenesis. TRIM31 regulates the immune response through MAVS and SYK, suppresses NLRP3-induced inflammasome activation and promotes autophagy in intestinal cells.[10-13] TRIM31 not only contributes significantly to cerebral ischemic injury by promoting degradation of TIGAR,[14] but also contributes to hypertensive nephropathy by promoting degradation of MAP3K7.[15] Through targeting Rhbdf2 in mouse hepato-

cytes, Trim31 alleviates non-alcoholic fatty liver disease.[16] In cases of aggressive AML, the mixed lineage leukemia 1 protein (MLL) has frequently been found to be fused with a partner (e.g., AF9).[17] Various investigations of MLL-AF9-induced AML have studied transcriptional regulators (e.g., HoxA9) and epigenetic modulators (e.g., Dot1L);[18,19] however, the study of post-translational regulation in MLL-AF9-mediated leukemogenesis remains scarce.

Cyclin-dependent kinase 8 (CDK8) is a cell-intrinsic regulator that functions conservatively in transcription, as a part of the CDK8-mediator complex.[20] The CDK8-mediator complex functions through releasing RNA polymerase II (RNAPII) from a paused state to start transcription.[21] The CDK8-mediator complex also functions as a tethering module in enhancement of gene transcription regulated by noncoding RNA.[22] During the innate immune response and inflammation, the mediator-associated kinase CDK8 plays a role as a negative regulator of interleukin-10.[23] *CDK8* has also been reported to act as an oncogene in both colon cancer[24,25] and melanoma.[26] In addition, the growth of AML cells can be inhibited by repressing CDK8 activity with small-molecule drugs.[27]

In this study, we found that *TRIM31* deletion leads to HSC proliferation and functional decline, while accelerating the initiation of leukemia. Mechanistically, TRIM31 functions as an E3 ligase of CDK8, and its deletion causes blockage of ubiquitin-mediated CDK8 degradation. The accumulation of CDK8 leads to enhanced expression of *PBX1* and *cyclin D1*. Potentially, an increase in E3 ligase activity of TRIM31 could be used as an anti-leukemia target because *TRIM31* deletion promotes the initiation and development of MLL-AF9-related AML.

Methods

Mice

TRIM31$^{+/-}$ mice[12] were a kind gift from Professor Chengjiang Gao of Shandong University and were produced by microinjecting transcription activator-like effector nuclease (TALEN) mRNA into fertilized eggs of mice with a C57BL/6 background. The *TRIM31*$^{-/-}$ mice were genotyped by sequencing polymerase chain reaction (PCR) fragments (250 bp) in the TALEN-targeting region, which was amplified from isolated genomic DNA from the mouse tail using the following primers: forward 5'-GGCCTTGGATTTCTGTACTTTCACATC-3' and reverse 5'-TGGGCCTGAACGTATTCTTATTCACAG-3'. Wild-type (WT) and *TRIM31*$^{-/-}$ mice aged 8-12 weeks were used in the experiments, except for those of marked age. The recipient mice, which were used in the competitive transplantation assays, were either CD45.1 mice or CD45.1/CD45.2 mice with a C57BL/6 background. The Animal Care and Ethics Committee at Jinan University approved all animal experiments in our study.

Flow cytometry and cell sorting

Bone marrow cells were freshly isolated from mice and incubated in a lineage cocktail of antibodies targeting CD4 (1:100, RM4-5), CD8 (1:100, 53-6.7), Ter-119 (1:100, TER-119), CD11b (1:150, M1/70), Gr-1 (1:150, RB6-8C5) and B220 (1:100, RA3-6B2) for 30 min. The cells were then washed and incubated in an antibody mix containing antibodies against CD34 (1:100, RAM34), and CD48 (1:200, HM48-1), CD45.2 (1:100, 104), IL-7R (1:100, A7R34), Flt3 (1:100, A2F10), CD150 (1:100, TC15-12F12.2), CD45.1 (1:100, A20), Sca1 (1:100, E13-161.7), c-Kit (1:100, ACK2), and CD16/32 (1:100, 93) and streptavidin. All antibodies were monoclonal and purchased from BD Biosciences. For cell sorting, the bone marrow cells were enriched with anti-antigen-presenting cell microbeads (Miltenyi Biotec) and then stained with antibodies for surface markers. Cell analysis and data acquisition were performed using an LSR Fortessa (BD Biosciences) cell analyzer, and cell sorting was carried out using an Aria 3 cell sorter (BD Biosciences). The data were analyzed using FlowJo software.

Cytokine stimulation of hematopoietic stem cells

HSC were sorted from the bone marrow of WT mice via flow cytometry, and then plated in SFEM medium supplemented with stem cell factor (10 ng/mL; Pepro Tech), thrombopoietin (10 ng/mL; Pepro Tech), interleukin-3 (10 ng/mL; Pepro Tech) and 100 U/mL penicillin/streptomycin. Cells were collected at 0 h, 24 h and 48 h time-points for the experiment.

MLL-AF9-mediated leukemia transformation assay

c-Kit^{+} cells were enriched from the bone marrow of WT and *TRIM31*$^{-/-}$ mice and then cultured in Iscove-modified Dulbecco medium containing 10% fetal bovine serum, 50 ng/mL stem cell factor, 10 ng/mL interleukin-3 and 10 ng/mL interleukin-6 overnight to stimulate cell proliferation. The next day, cells were transduced with retrovirus encoding MLL-AF9. After 72 h, cells were harvested and GFP^{+} cells were sorted by an Aria 3 Sorter. GFP^{+} cells ($5x10^{4}$) were transplanted together with $5x10^{5}$ bone marrow cells into lethally irradiated recipients. Mice were monitored for MLL-AF9 AML development. Five thousand GFP^{+} cells were sorted and plated in colony-forming units assay using MethoCult M3434 (STEMCELL Technologies) media for 10 days before colony counting.

Results

TRIM31 deletion impairs hematopoietic stem and progenitor cell homeostasis

E3 ligase regulates the cell cycle efficiently through precise control of cell cycle factors (e.g., CDK and cyclin proteins) at the protein level. An increasing number of studies

have shown that the E3 ligase function of TRIM proteins plays an essential role in tumorigenesis;[28] however, its role in the hematopoietic system and leukemia initiation has rarely been studied. Real-time PCR revealed that the mRNA level of *TRIM31* is reduced significantly after stimulation of HSC proliferation and differentiation (*Online Supplementary Figure S1A*), which indicates high expression of *TRIM31* may play a potential role in the cell cycle control of HSC. To determine the function of TRIM31 in regulating HSC, *TRIM31* knockout mice were created[12] (*Online Supplementary Figure S1B, C*) and analyzed by using fluorescence activated cell sorting (FACS). In the hematopoietic system, the cellularity of *TRIM31*$^{-/-}$ bone marrow and Lin$^-$ cells remained similar to that of WT mice (*Online Supplementary Figures S1D-F*); however, the number of LK (Lin$^-$Sca-1$^-$c-Kit$^+$) progenitor cells decreased significantly (*Online Supplementary Figure S1G, H*). In the bone marrow of *TRIM31*$^{-/-}$ mice, FACS analysis revealed higher numbers of common lymphoid progenitors (CLP) and lower numbers of common myeloid progenitor (CMP), but no variation in the number of granulocyte/monocyte progenitors (GMP) (Figure 1A, B; *Online Supplementary Figure S1G, I-K*). A more than 2-fold increase was also shown in both the absolute number and frequency of LSK (Lin$^-$

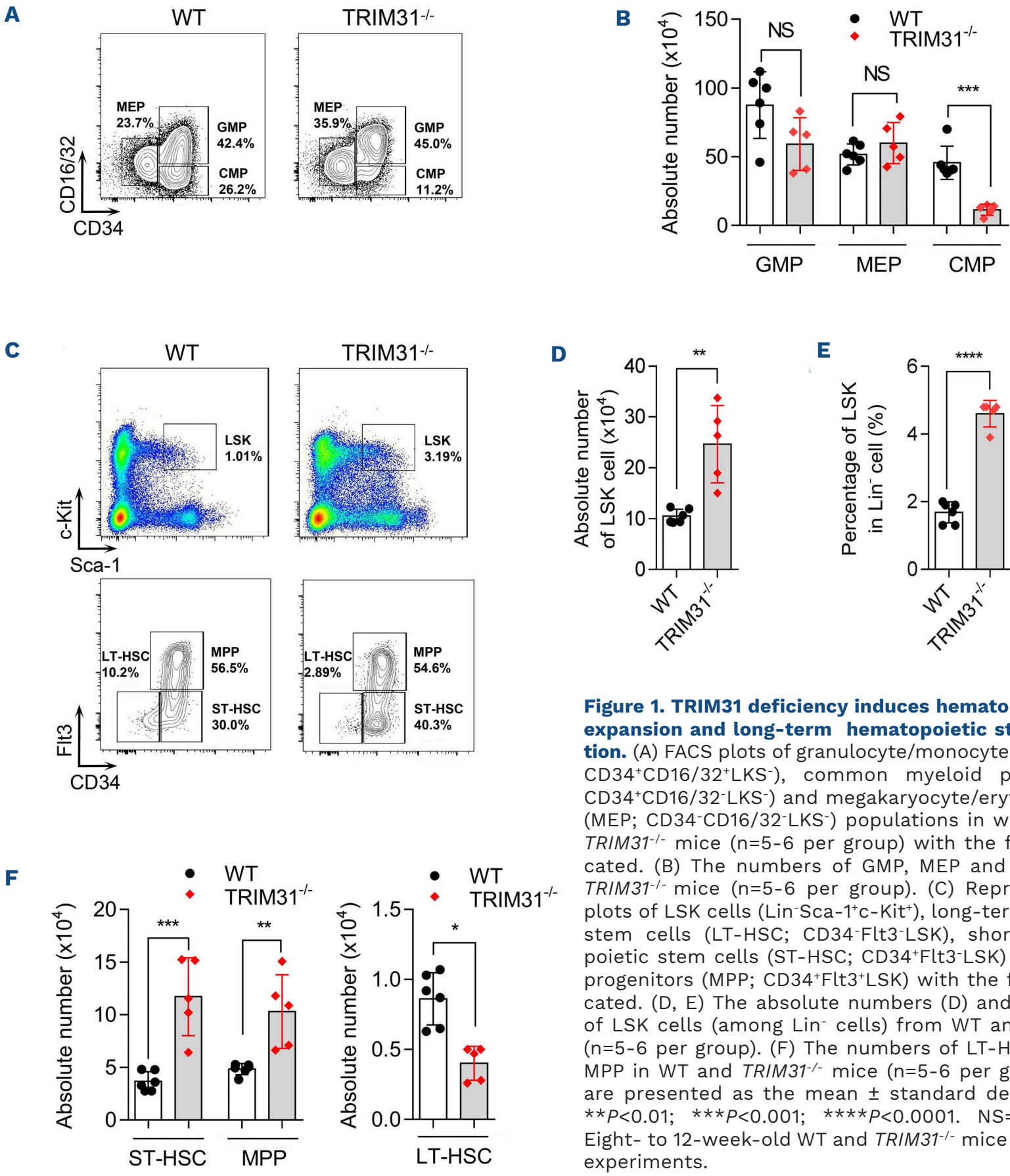

Figure 1. TRIM31 deficiency induces hematopoietic stem cell expansion and long-term hematopoietic stem cell exhaustion. (A) FACS plots of granulocyte/monocyte progenitor (GMP; CD34$^+$CD16/32$^+$LKS$^-$), common myeloid progenitor (CMP; CD34$^+$CD16/32$^-$LKS$^-$) and megakaryocyte/erythroid progenitor (MEP; CD34$^-$CD16/32$^-$LKS$^-$) populations in wildtype (WT) and *TRIM31*$^{-/-}$ mice (n=5-6 per group) with the frequencies indicated. (B) The numbers of GMP, MEP and CMP in WT and *TRIM31*$^{-/-}$ mice (n=5-6 per group). (C) Representative FACS plots of LSK cells (Lin$^-$Sca-1$^+$c-Kit$^+$), long-term hematopoietic stem cells (LT-HSC; CD34$^-$Flt3$^-$LSK), short-term hematopoietic stem cells (ST-HSC; CD34$^+$Flt3$^-$LSK) and multipotent progenitors (MPP; CD34$^+$Flt3$^+$LSK) with the frequencies indicated. (D, E) The absolute numbers (D) and percentages (E) of LSK cells (among Lin$^-$ cells) from WT and *TRIM31*$^{-/-}$ mice (n=5-6 per group). (F) The numbers of LT-HSC, ST-HSC, and MPP in WT and *TRIM31*$^{-/-}$ mice (n=5-6 per group). All results are presented as the mean ± standard deviation. **P*<0.05; ***P*<0.01; ****P*<0.001; *****P*<0.0001. NS=not significant. Eight- to 12-week-old WT and *TRIM31*$^{-/-}$ mice were used in the experiments.

Sca-1$^+$c-Kit$^+$) cells in *TRIM31*$^{-/-}$ bone marrow (Figure 1C-E). To further characterize the composition of the LSK population, CD34 and Flt3 markers were used to distinguish long-term HSC (LT-HSC; CD34$^-$Flt3$^-$ LSK), short-term HSC (ST-HSC; CD34$^+$Flt3$^-$ LSK), and multipotent progenitors (MPP; CD34$^+$Flt3$^+$ LSK). In *TRIM31*$^{-/-}$ bone marrow, the numbers of ST-HSC and MPP increased dramatically, while the absolute number of LT-HSC decreased significantly (Figure 1C, F), which is probably attributable to stem cell exhaustion.

In bone marrow, *TRIM31* depletion resulted in a significant decrease of B lymphocyte number (*Online Supplementary Figure S2A, B*), while the difference in peripheral blood was minimal (*Online Supplementary Figure S2C*). During erythrocyte development, the percentage of E3 (TER119$^+$CD71^{mid}) cells increased dramatically in *TRIM31*$^{-/-}$ mice (*Online Supplementary Figure S2D, E*). In addition, the spleen was hypertrophic in *TRIM31*$^{-/-}$ mice (*Online Supplementary Figure S3A, B*), and the hypertrophic spleen contained a higher percentage of LSK cells (*Online Supplementary Figure S3C*), indicating that *TRIM31* deletion may cause malfunction of the spleen. Consistently, the composition of B cells decreased while the proportion of myeloid cells increased in *TRIM31*$^{-/-}$ mouse spleens (*Online Supplementary Figure S3D*). Overall, *TRIM31* deletion impaired HSC homeostasis, causing harm to the cellularity of LT-HSC, ST-HSC, MPP and LSK cells, which further resulted in abnormal regulation of progenitors, such as CMP and CLP.

Loss of *TRIM31* impairs hematopoietic stem cell function of reconstitution capacity

To evaluate the self-renewal and differentiation capacity of LT-HSC *in vivo*, we performed a competitive LT-HSC transplantation experiment. As donor cells, 300 LT-HSC were sorted from WT and *TRIM31*$^{-/-}$ mice and transplanted into lethally irradiated recipient mice together with 3x10^5 bone marrow competitors (*Online Supplementary Figure S3E*). The percentage of donor-derived cells (chimerism) in peripheral blood was analyzed every 4 weeks. The chimerism of *TRIM31*$^{-/-}$ cells in peripheral blood was much lower than that of WT cells (Figure 2A). After 16 weeks, bone marrow analysis of chimeric mice showed that donor-derived *TRIM31*$^{-/-}$ LSK cells were also greatly reduced in comparison to donor-derived WT cells (Figure 2B). Further analysis revealed that the chimerism of *TRIM31*$^{-/-}$ cells was significantly decreased at the LT-HSC, ST-HSC and MPP (MPP2 and MPP3) levels (Figure 2B). For consecutive transplantation, 1x10^6 chimeric bone marrow cells were re-transplanted into secondary recipient mice (*Online Supplementary Figure S3E*). As in the first round of transplantation, the percentage of donor-derived *TRIM31*$^{-/-}$ cells in peripheral blood dropped further, while that of donor-derived WT cells remained nearly the same. The peripheral blood chimerism of *TRIM31*$^{-/-}$-derived cells was almost zero at 28 weeks after transplantation, while that of WT-derived cells remained approximately 50% (Figure 2A). Bone marrow analysis after the second transplantation showed that LSK chimerism was dramatically decreased in *TRIM31*$^{-/-}$-derived cells in comparison to WT-derived cells (Figure 2C). Furthermore, chimerism analysis of LT-HSC, ST-HSC and MPP showed dramatic reductions in *TRIM31*$^{-/-}$-derived cells (Figure 2C). The chimerism in T lymphocytes, B lymphocytes and myeloid cells in peripheral blood was also clearly decreased following both the first and second transplants (Figure 2D-F).

To confirm the results of LT-HSC transplantation, a competitive LSK transplantation experiment was performed using 4,000 LSK cells sorted from WT and *TRIM31*$^{-/-}$ mice, together with 1x10^6 competitive cells (*Online Supplementary Figure S4A*). As for the LT-HSC transplantation, peripheral blood chimerism was analyzed every 4 weeks, and the percentage of donor-derived *TRIM31*$^{-/-}$ cells in peripheral blood was significantly decreased in comparison to that of donor-derived WT cells (*Online Supplementary Figure S4B*). Bone marrow analysis also indicated that chimerism of donor-derived LSK cells was significantly reduced in *TRIM31*$^{-/-}$-derived cells (*Online Supplementary Figure S4C*). This reduction in chimerism was simultaneously observed at the LT-HSC, ST-HSC and MPP levels in *TRIM31*$^{-/-}$-derived cells (*Online Supplementary Figure S4D, E*). Additionally, T lymphocytes, B lymphocytes, and myeloid cells all displayed drastic reductions in chimerism (*Online Supplementary Figure S4F-H*). To exclude the effect of *TRIM31* deletion in the stem cell niche, 4,000 WT LSK cells were sorted and transplanted into WT and *TRIM31*$^{-/-}$-recipient mice. No statistically significant difference of donor-derived LSK chimerism was shown between WT and *TRIM31*$^{-/-}$-recipient mice (*Online Supplementary Figure S4I, J*). In summary, after serial competitive transplantation, *TRIM31* deletion significantly reduced peripheral blood chimerism and bone marrow chimerism at the levels of LSK cells, LT-HSC, ST-HSC, and MPP, indicating that *TRIM31* deletion impairs the reconstitution ability of HSC.

TRIM31 deficiency promotes the proliferation of hematopoietic stem cells and reduces their self-renewal capacity under stress

To ascertain the underlying reasons for hematopoietic stem and progenitor cell alterations in *TRIM31*$^{-/-}$ mice, a BrdU incorporation assay was performed. *TRIM31* deletion induced a significant increase of BrdU-positive cells both at the LSK cell and LT-HSC levels, indicating that *TRIM31* deletion promotes proliferation of HSC (Figure 3A, B). This indication was also supported by the decrease of Ki67-negative staining in *TRIM31*$^{-/-}$ cells (*Online Supplementary Figure S5A-D*). Conditions of stress, such as 5-fluorouracil (5-FU) treatment, could cause apoptosis of cycling HSC, whereas quiescent HSC might remain viable.[29] To detect

the stress effect of *TRIM31* deficiency on HSC, we challenged *TRIM31*$^{-/-}$ mice with sequential 5-FU administration. *TRIM31*$^{-/-}$ mice challenged with sequential 5-FU treatment died much earlier than WT controls (Figure 3C), demonstrating that *TRIM31*-null HSC were more activated. 5-FU treatment was also used to quantify cell self-renewal capacity. Analysis of the results at 6 days after 5-FU treatment revealed that *TRIM31*$^{-/-}$ mice had considerably fewer LSK cells than WT mice. Subsequent analysis demonstrated that the numbers of LT-HSC, ST-

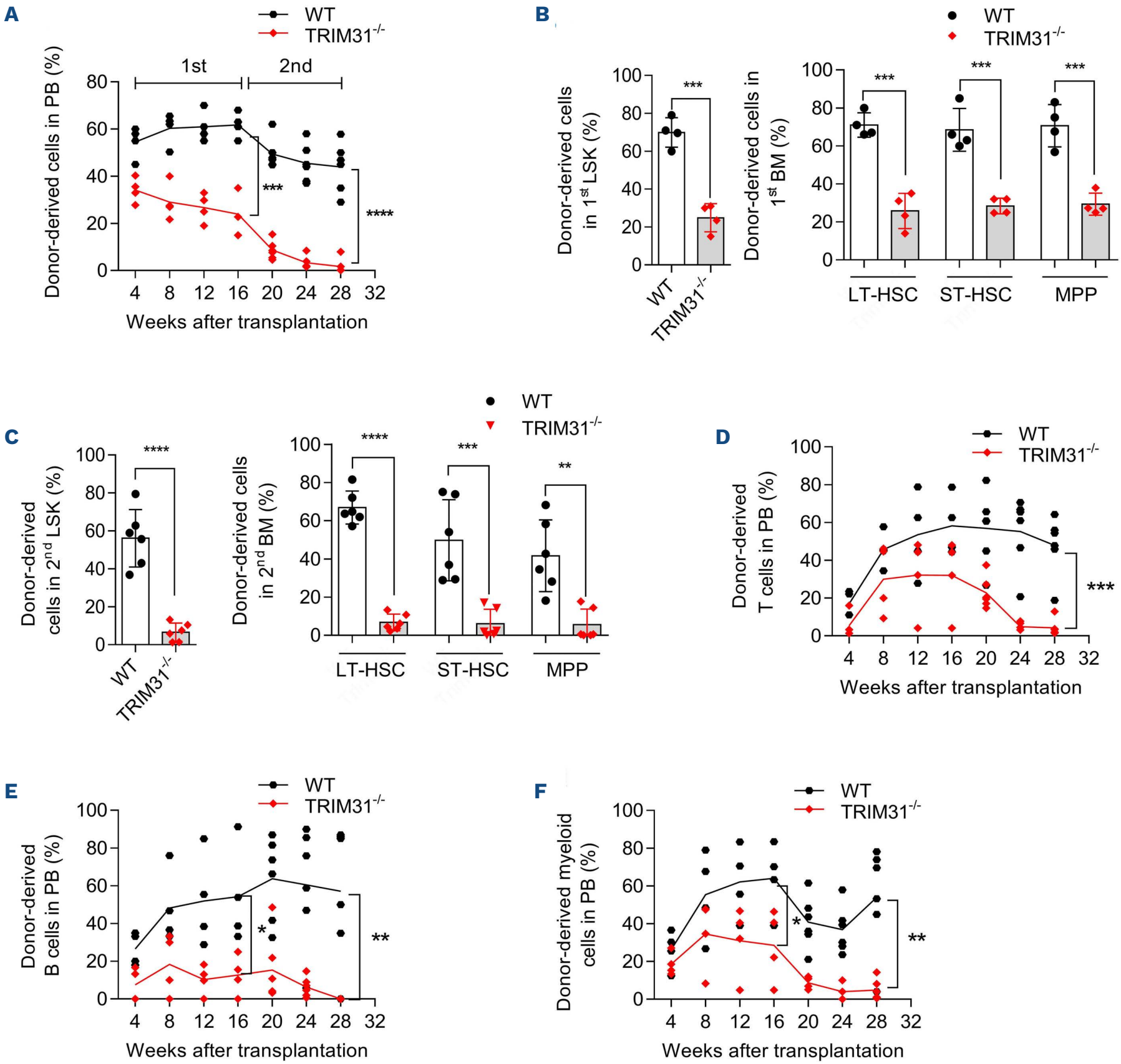

Figure 2. Loss of *TRIM31* impairs long-term hematopoietic stem cell function. (A) The percentage of donor-derived peripheral blood cells at the indicated time-points in the serial competitive transplantation assay is shown (1st, for the first competitive transplantation, 4 recipient mice per group; 2nd, for the second competitive transplantation, 6 recipient mice per group). (B) Percentages of donor-derived LSK (Lin$^-$Sca-1$^+$c-Kit$^+$) cells, long-term hematopoietic stem cells (LT-HSC; CD48$^-$CD150$^+$Flt3$^-$LSK), short-term hematopoietic stem cells (ST-HSC; CD48$^-$CD150$^-$Flt3$^-$LSK) and multipotent progenitors (MPP; CD48$^+$Flt3$^-$LSK) 16 weeks after the first transplantation are shown (n=4 per group). (C) Percentages of donor-derived LSK cells, LT-HSC, ST-HSC and MPP cells 12 weeks after secondary transplantation are shown (n=6 per group). (D-F) Two-round serial transplantation was conducted using 300 purified LT-HSC cells along with 3x10^5 fresh competitors each time. Chimerism of T, B and myeloid cells in peripheral blood is shown at the indicated time-points after transplantation. All results are presented as the mean ± standard deviation. ***P*<0.01; ****P*<0.001; *****P*<0.0001. Eight- to 12-week-old wildtype and *TRIM31*$^{-/-}$ mice were used in the experiments. WT: wildtype; PB: peripheral blood; BM: bone marrow.

HSC and MPP after 5-FU administration were all substantially reduced in *TRIM31*$^{-/-}$ mice compared to the numbers in WT mice (Figure 3D, E). To further confirm the defect caused by *TRIM31* deletion, a single-colony formation assay was used to quantify the ability of HSC to proliferate and differentiate *in vitro*. In *TRIM31*$^{-/-}$ LT-HSC, the number of large colonies was significantly decreased, indicating that the self-renewal ability of LT-HSC was impaired after long-term activation (Figure 3F). In short, *TRIM31* deletion induces HSC proliferation *in vivo* and

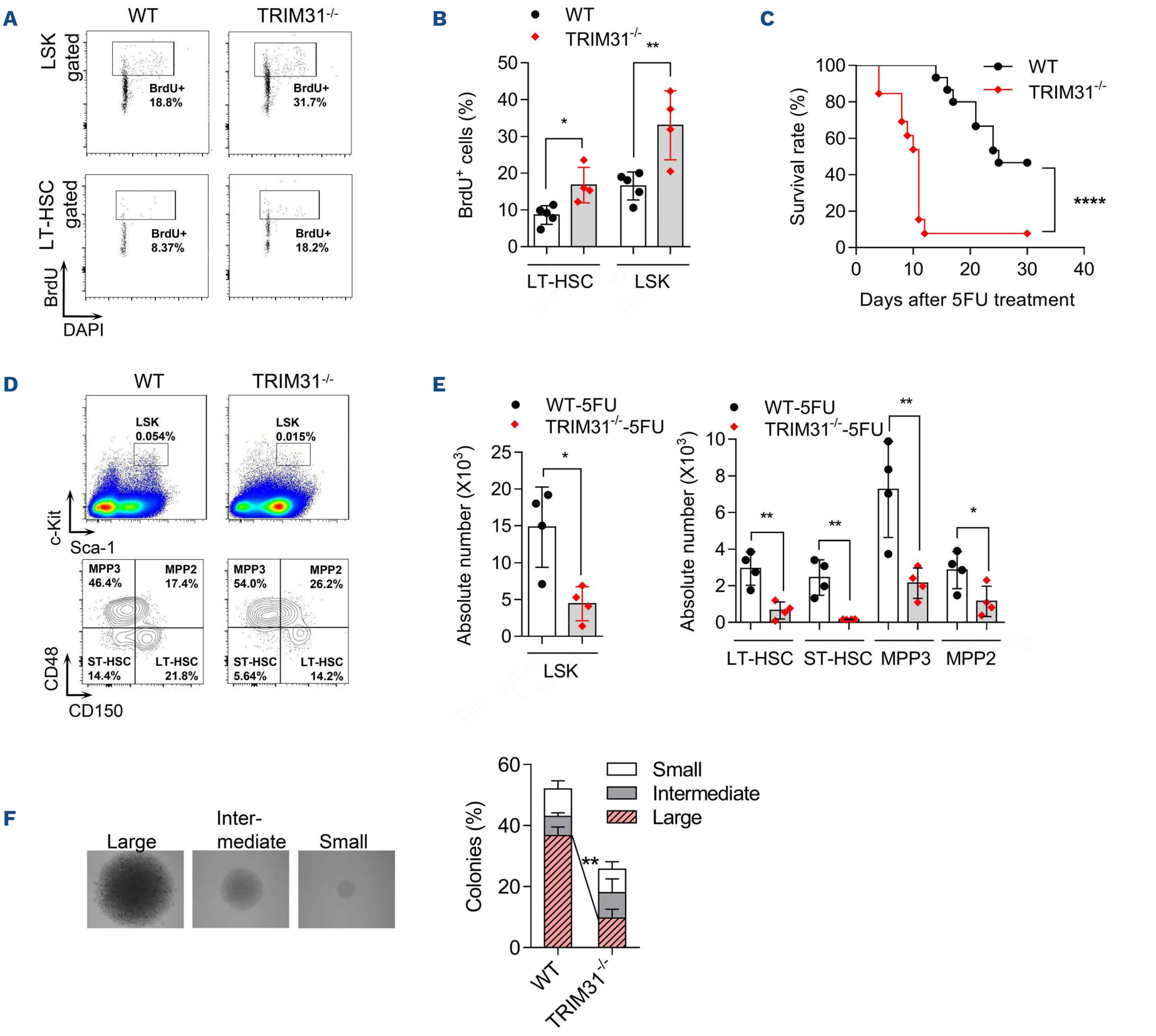

Figure 3. *TRIM31* deletion leads to enhanced hematopoietic stem cell proliferation and reduced self-renewal capacity under stress. (A) Representative FACS plots showing the proliferation analysis in long-term hematopoietic stem cells (LT-HSC; CD48^{-} CD150^{+}Flt3^{-} LSK) and LSK (Lin-Sca-1^{+}c-Kit^{+}) cells. The percentages of BrdU-positive cells are shown. (B) The percentages of BrdU-positive cells among LT-HSC and LSK cells from wildtype (WT) and *TRIM31*$^{-/-}$ mice after long-term BrdU labeling (10 days) (n=4-5 per group). (C) Survival curves of WT and *TRIM31*$^{-/-}$ mice following sequential 5-fluoruracil (5FU) treatment (n=13 per group). 5FU was injected into mice once a week for a total of two injections. (D) Representative FACS plots of LSK, LT-HSC, short-term hematopoietic stem cells (ST-HSC; CD48^{-}CD150^{-}Flt3^{-} LSK) and multipotent progenitors (MPP2; CD48^{+}CD150^{+}Flt3^{-} LSK and MPP3; CD48^{+}CD150^{-}Flt3^{-} LSK) 6 days after 5FU treatment. (E) The absolute numbers of LT-HSC, ST-HSC, MPP2 and MPP3 cells in WT and *TRIM31*$^{-/-}$ mice after 5FU treatment (n=4 per group). (F) Representative images of large, intermediate and small colonies are shown. The percentages of colonies formed after 14 days of culture of single LT-HSC sorted from WT and *TRIM31*$^{-/-}$ mice are shown (n=3 per group). All results are presented as the mean ± standard deviation. **P*<0.05; ***P*<0.01; *****P*<0.0001. Eight- to 12-week-old WT and *TRIM31*$^{-/-}$ mice were used in the experiments.

leads to a functional decline of self-renewal ability under a condition of stress.

TRIM31 deletion accelerates leukemia initiation in a model of MLL-AF9-induced acute myeloid leukemia

To evaluate whether the accelerated proliferation of *TRIM31*$^{-/-}$ hematopoietic cells is related to leukemia, a database analysis was carried out and revealed that low expression of *TRIM31* was associated with poor AML survival (Figure 4A, B; *Online Supplementary Figure S5E*). Among patients with various types of AML, *TRIM31* expression was relatively lower in those with *MLL* rearrangements (*Online Supplementary Figure S5F*). Therefore, a murine AML model driven by the human oncogene *MLL-AF9* was used to investigate the role of TRIM31 in leukemia initiation and development.[30] c-Kit^{+} cells were enriched from bone marrow of WT and *TRIM31*$^{-/-}$ mice, and then transduced with *MLL-AF9* retrovirus (*Online Supplementary Figure S6A*). I*n vitro*, a surrogate functional examination using methylcellulose medium revealed that TRIM31-null MLL-AF9 primary transformed cells had significantly increased colony-forming capability (*Online Supplementary Figure S6B*). During primary plating and second plating, the numbers of colonies and total cells were markedly higher for MLL-AF9-converted *TRIM31*$^{-/-}$ cells than for WT cells (*Online Supplementary Figure S6C, D*). To assess leukemogenesis *in vivo*, *MLL-AF9* retrovirus-transduced WT and *TRIM31*$^{-/-}$ cells were sorted and transplanted into lethally irradiated recipient mice after which the development of AML was monitored (*Online Supplementary Figure S6A*). The frequency of L-GMP (Lin^{-}Sca1^{-}c-Kit^{+}CD34^{+}CD16/32^{+}) cells was reported as leukemia-initiating cells in the MLL-AF9-induced leukemia.[31] A higher frequency of L-GMP was detected in the bone marrow of *TRIM31*$^{-/-}$ donors than in WT donors (Figure 4C). In peripheral blood, the frequency of GFP^{+} leukemic cells was significantly higher in *TRIM31*$^{-/-}$ donors than in WT ones (Figure 4D). Meanwhile, recipient mice that received MLL-AF9-transduced *TRIM31*$^{-/-}$ donor cells had a significantly shorter overall survival than WT mice (Figure 4E). Moreover, after the L-GMP cells from leukemia mice had been sorted and transplanted, the disparity in overall survival of mice receiving grafts from WT or *TRIM31*$^{-/-}$ donors increased dramatically (Figure 4F). Taking into consideration the uniform expression, copies of *MLL-AF9* fusion gene and mean fluorescent intensity of GFP in both WT and *TRIM31*$^{-/-}$ donor cells (*Online Supplementary Figure S6E-J*), these data collectively support that *TRIM31* deletion accelerated the initiation and development of MLL-AF9-induced AML.

TRIM31 functions as an E3 ligase of CDK8 and regulates its ubiquitin-mediated degradation

The selected TRIM31 interacting protein candidates after mass spectrometry analysis are summarized. Through MAVS and NLRP3, TRIM31 plays a critical role in macrophages and intestinal cells.[15-17] In order to identify the underlying mechanism and the functional substrate of TRIM31 in hematopoietic cells, we performed mass spectrometry (MS) on WT cells, with *TRIM31*$^{-/-}$ cells used as the negative control (*Online Supplementary Figure S7A*). Several TRIM31 interacting protein candidates in WT cells were selected after MS (*Online Supplementary Table S1*). Interestingly, FACS analysis showed that the median fluorescence intensity of CDK8 was dramatically increased in LT-HSC, LSK cells and Lin^{-} cells from *TRIM31*$^{-/-}$ mice, whereas no difference in the mean fluorescence intensity of EIF5A and Cdkn2a was detected between WT and *TRIM31*$^{-/-}$ mice (Figure 5A; *Online Supplementary Figure S7B, C*). The increased CDK8 level in cells from *TRIM31*$^{-/-}$ mice was verified by western blot (Figure 5B). Moreover, the cell cycle regulator cyclin D1 was strongly upregulated in *TRIM31*$^{-/-}$ cells (Figure 5B), and this upregulation was accompanied by an increase in its interaction partner CDK6 (*Online Supplementary Figure S7D*), which may be due to cell proliferation. To verify whether CDK8 is a direct ubiquitin substrate of TRIM31, we performed a co-immunoprecipitation assay of CDK8 antibody using WT and *TRIM31*$^{-/-}$ cells, which were treated with a proteasomal inhibitor (MG132) before cell lysis. The level of ubiquitination of CDK8, but not of CDK6, was reduced dramatically in *TRIM31*$^{-/-}$ cells (Figure 5C; *Online Supplementary Figure S7E*), indicating that CDK8 is a ubiquitin substrate of the E3 ligase, TRIM31. Furthermore, the successful pulling down of TRIM31 and CDK8 together confirmed a direct protein interaction between them (Figure 5D). Surprisingly, CDK8 could pull down and co-localize with cyclin D1 (Figure 5D; *Online Supplementary Figure S7F*), suggesting that cyclin D1 might function together with CDK8 in hematopoietic cells. Importantly, upregulation of CDK8 and cyclin D1 was observed in *TRIM31*$^{-/-}$ mouse spleens (Figure 5E), and the level of CDK8 protein was also enhanced in *TRIM31*$^{-/-}$ leukemia and L-GMP cells (Figure 5F). In brief, CDK8 accumulation in hematopoietic and leukemia cells was caused by deletion of its E3 ligase TRIM31 and eventually led to enhanced expression of the cell cycle regulator *cyclin D1*.

Genetic knockdown of *CDK8* or *cyclin D1* rescues the defects in *TRIM31*$^{-/-}$ hematopoietic stem cells

To confirm that the functional decline in stem cells in *TRIM31*$^{-/-}$ mice was attributable to upregulation of CDK8, an experiment of inhibition of CDK8 was performed. LY2857785 is a type I reversible and competitive ATP kinase inhibitor of both CDK8 and CDK9.[32] After the administration of LY2857785 to WT and *TRIM31*$^{-/-}$ mice for 2 weeks, LT-HSC were sorted and transplanted together with competitors into recipient mice (*Online Supplementary Figure S8A*). Eight to 10 weeks later, FACS analysis

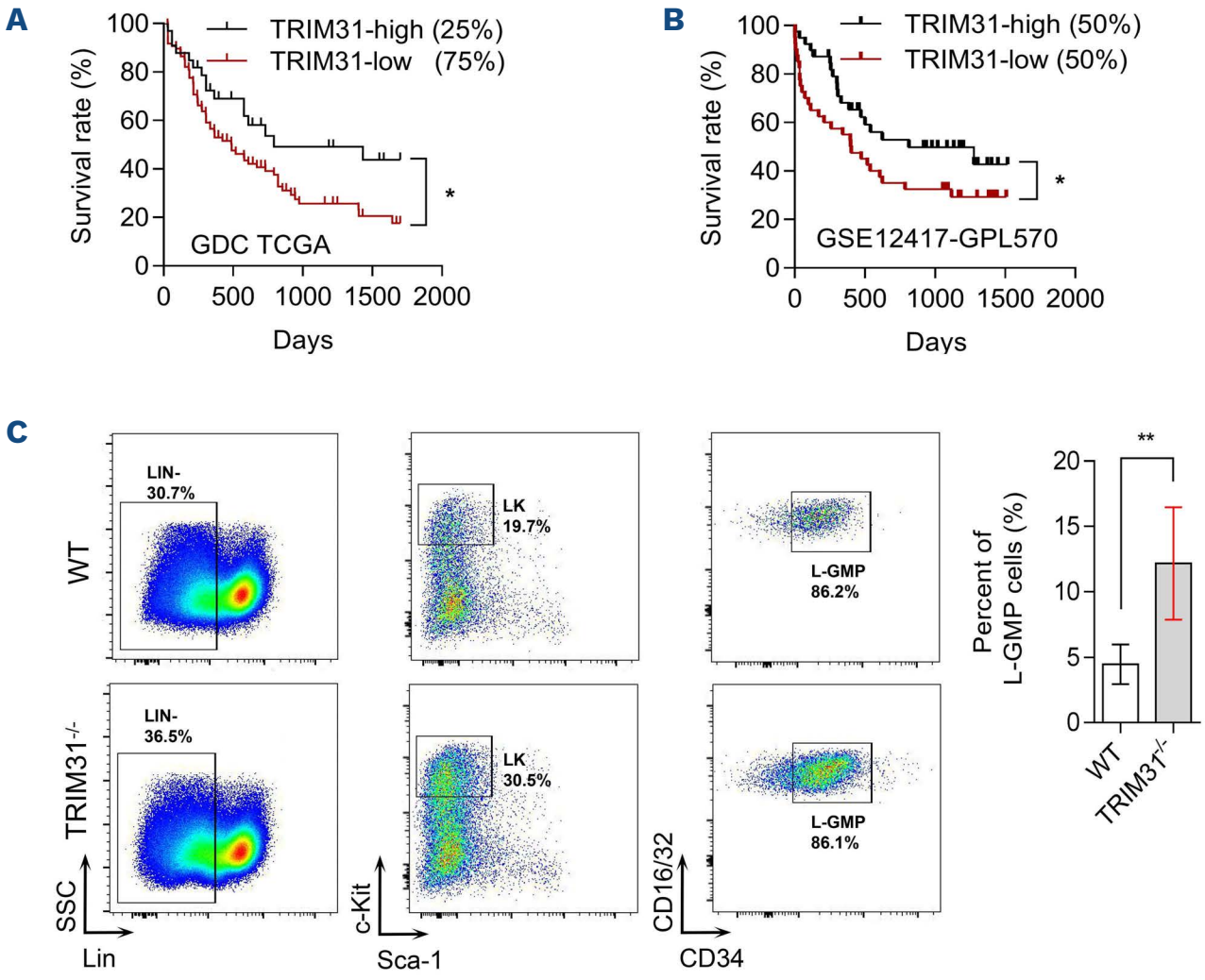

Figure 4. *TRIM31* deletion accelerated leukemia initiation in an MLL-AF9-induced mouse model. (A) Kaplan-Meier survival curve analysis of The Cancer Genome Atlas dataset (*https://xenabrowser.net/*) comparing the acute myeloid leukemia (AML) patients with high (n=33) *versus* low (n=99) *TRIM31* expression. (B) Kaplan-Meier survival curve analysis of the GSE12417 dataset comparing AML patients with high (n=39) *versus* low (n=40) *TRIM31* expression. (C) Representative FACS plots showing the percentages of L-GMP cells ($Lin^-Sca1^-c\text{-}Kit^+CD34^+CD16/32^+$) in the bone marrow (BM) of wildtype (WT) and *TRIM31*$^{-/-}$ recipient mice (n=4-6 per group). (D) Representative FACS plots showing the percentages of GFP^+ cells and myeloid cells in the peripheral blood (PB) of WT and *TRIM31*$^{-/-}$ recipient mice (n=4-6 per group). (E) Survival curves of mice transplanted with MLL-AF9 WT or *TRIM31*$^{-/-}$ leukemic cells (n=5 per group). (F) Survival curves of mice transplanted with 5,000 WT or *TRIM31*$^{-/-}$ L-GMP cells (n=5 per group). All results are presented as the mean ± standard deviation. **P*<0.05; ***P*<0.01. Eight- to 12-week-old WT and *TRIM31*$^{-/-}$ mice were used in the experiment. GDC: Genomic Data Commons; TCGA: The Cancer Genome Atlas; SSC: side scatter; FSC: forward scatter; GFP: green fluorescent protein.

showed that the treatment of *TRIM31*$^{-/-}$ mice with a CDK8 inhibitor caused enhancement of peripheral blood LSK and LT-HSC chimerism, while no difference was shown in the control group (Figure 6A, B; *Online Supplementary Figure S8B-D*). To inhibit CDK8 more specifically, LT-HSC from *TRIM31*$^{-/-}$ mice were infected with lentivirus containing GFP-labeled shRNA against *CDK8* and transplanted into recipient mice. Twelve, 16 and 20 weeks later, peripheral blood analysis showed that the percentage of donor-derived cells was dramatically increased in the *CDK8* knockdown group (Figure 6C). A similar phenomenon was also found in donor-derived LSK cells after bone marrow

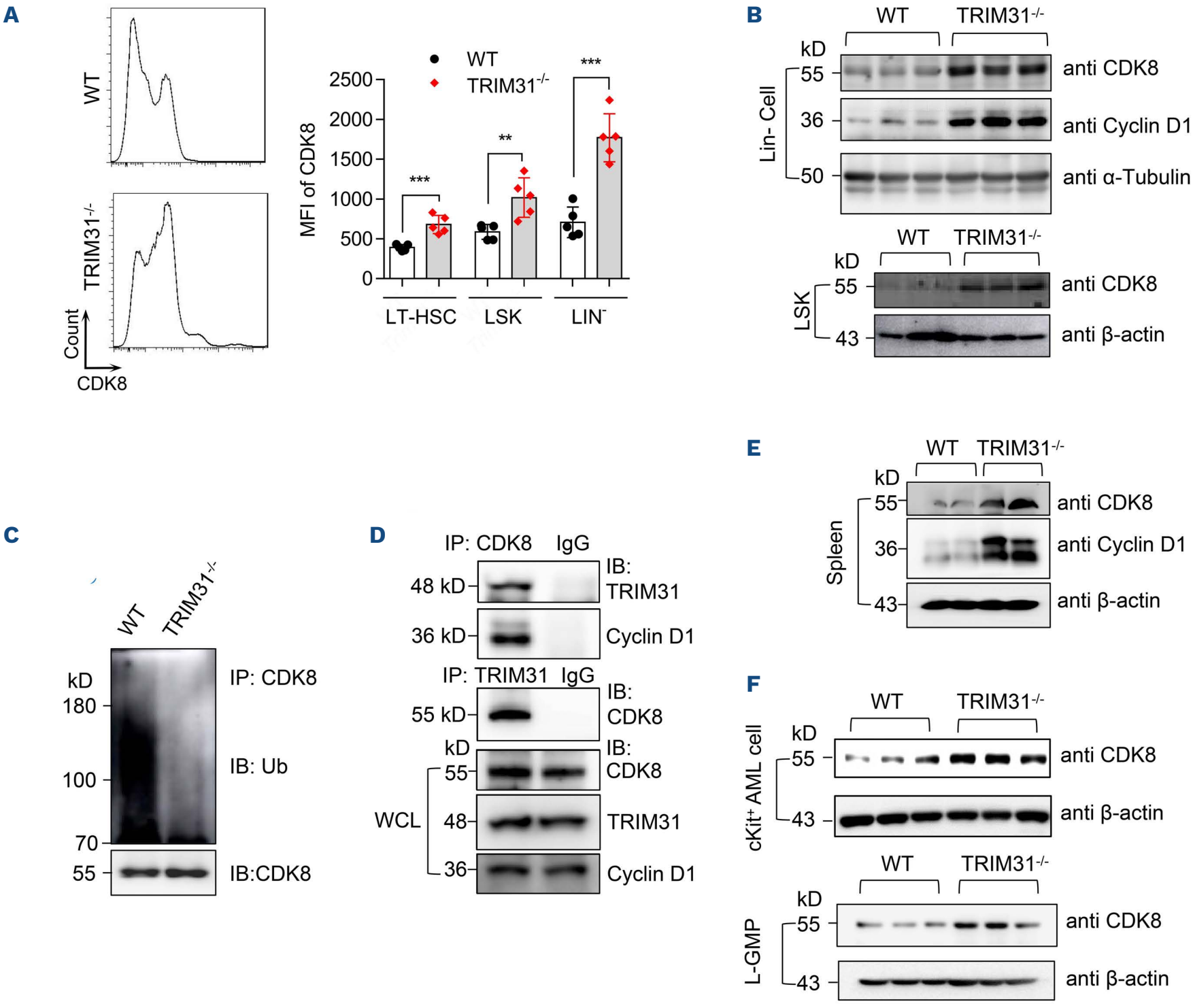

Figure 5. Accumulation of CDK8 and upregulation of cyclin D1 were caused by *TRIM31* deletion. (A) Representative FACS plots of CDK8 mean fluorescence intensity (MFI) in Lin$^-$ cells from wildtype (WT) and *TRIM31*$^{-/-}$ mice. The MFI of CDK8 in long-term hematopoietic stem cells (LT-HSC; CD48$^-$CD150$^+$Flt3$^-$ LSK), LSK cells (Lin$^-$Sca-1$^+$c-Kit$^+$) and Lin$^-$ cells from WT and *TRIM31*$^{-/-}$ mice is shown (n=5 per group). (B) Immunoblot (IB) of cyclin D1 and CDK8 in the whole cell lysate (WCL) of Lin$^-$ cells from WT and *TRIM31*$^{-/-}$ mice. α-tubulin was used as a loading control (n=3 per group). IB of CDK8 in the WCL of LSK cells from WT and *TRIM31*$^{-/-}$ mice. β-actin was used as a loading control (n=3 per group). (C) Ubiquitination assay of CDK8 in the whole cell lysate of Lin$^-$ cells from WT and *TRIM31*$^{-/-}$ mice treated with a proteasomal inhibitor (MG132). IB against ubiquitin was performed with the immunoprecipitation (IP) assay precipitate of anti-CDK8 and CDK8 from WCL used as a loading control. (D) IP of anti-CDK8 and anti-TRIM31 was performed on the WCL of Lin$^-$ cells from WT mice; IP of anti-IgG was used as a control. IB against TRIM31, cyclin D1 and CDK8 was performed with the IP assay precipitate and the WCL of Lin$^-$ cells, which was used as a loading control. (E) IB of cyclin D1 and CDK8 in WCL of spleens from WT and *TRIM31*$^{-/-}$ mice. β-actin was used as a loading control (n=2 per group). (F) IB of CDK8 in the WCL of c-Kit+ cells from recipient mice transplanted with MLL-AF9 WT and *TRIM31*$^{-/-}$ cells. β-actin was used as a loading control (n=3-4 per group). IB of CDK8 in the WCL of L-GMP cells from recipient mice transplanted with MLL-AF9 WT and *TRIM31*$^{-/-}$ cells. β-actin was used as a loading control (n=3 per group). All results are presented as the mean ± standard deviation. ***P*<0.01; ****P*<0.001. Eight- to 12-week-old WT and *TRIM31*$^{-/-}$ mice were used in the experiments. Ub: ubiquitin.

analysis (Figure 6D; *Online Supplementary Figure S8E-G*). The above results demonstrate that knockdown of *CDK8* in *TRIM31*$^{-/-}$ LT-HSC could lead to enhanced stem cell function, which might be due to the prevention of LT-HSC exhaustion (Figure 6E, F). In addition, knockdown of *cyclin D1* in *TRIM31*$^{-/-}$ LT-HSC also resulted in an increased percentage of donor-derived cells (*Online Supplementary Figure S9A-F*), which was similar to the effects of overexpression of TRIM31 (*Online Supplementary Figure S10A-C*), showing that TRIM31 and cyclin D1 may function in the same pathway (*Online Supplementary Figure S9G*). Meanwhile, overexpression of *TRIM31* caused reduced colony formation in WT MLL-AF9 leukemia cells (*Online Supplementary Figure S10D*). In short, TRIM31 functions through the CDK8/cyclin D1 pathway, which also inhibits the development of MLL-AF9, since both pharmaceutical inhibition of CDK8 and genetic knockdown of *CDK8* and *cyclin D1* rescued the functional defects in *TRIM31*$^{-/-}$ HSC.

CDK8 regulates the expression of *cyclin D1* through transcriptional factor PBX1

The CDK8-mediator is a large macromolecular complex comprising four modules, the head, middle, tail, and kinase modules, which consists of CDK8 and three other factors: Med12, Med13 and cyclin C.[33] CDK8, MED12 and RNAPII were found to bind the promotor region of the transcriptional factor PBX1 after analysis of chromatin immunoprecipitation (ChIP) sequencing data (GEO dataset: GSE128242) (Figure 7A).[34] *PBX1* is a proto-oncogene in the hematopoietic system, and its loss results in exhaustion of LT-HSC and defects in HSC maintenance and function.[35] Meanwhile, the upregulation of *PBX1* promotes cell proliferation.[36] Through ChIP-quantitative PCR, CDK8 was verified to be enriched at the promoter region of *PBX1* (Figure 7B). To determine the underlying mechanism of CDK8 regulation, quantitative PCR analysis of *cyclin D1* and *PBX1* was performed. Both mRNA expression levels of *cyclin D1* and *PBX1* were enhanced in *TRIM31*$^{-/-}$ hematopoietic and L-GMP cells (Figure 7C), which was verified at the protein level by western blot (Figure 7D). In order to further determine the relationship between CDK8, PBX1 and cyclin D1, *CDK8* was knocked down and overexpressed in NIH/3T3 mouse fibroblasts. The transcriptional expression of *PBX1* and the mRNA expression of *cyclin D1* were regulated through the mRNA level of *CDK8* (Figure 7E). Similarly, the downregulation of *PBX1* caused by knockdown of *CDK8* was also shown in hematopoietic cells (Figure 7F). Moreover, the changes in *PBX1* directly regulated the expression of *cyclin D1*, indicating that PBX1 is located upstream of cyclin D1 (*Online Supplementary Figure S11A*). Functionally, knockdown of *PBX1* in *TRIM31*$^{-/-}$ LT-HSC resulted in an increased percentage of donor-derived cells (*Online Supplementary Figure S11B-F*), and knockdown of *TRIM31* resulted in increased expression of *PBX1* and *cyclin D1* in THP1 cells (*Online Supplementary Figure S11G*), implying that TRIM31 and PBX1 may act in the same pathway. In concordance with our quantitative PCR data, the expression of *PBX1* and *cyclin D1* in primary AML patients was correlated with *CDK8* expression (*Online Supplementary Figure S12A, B*). Furthermore, *cyclin D1* was significantly increased in patients with higher *PBX1* expression (*Online Supplementary Figure S12C*). In general, CDK8 regulates the expression of *cyclin D1* through the transcriptional factor PBX1.

Discussion

Ubiquitin E3 ligases are vital regulators of the hematopoietic system, and their absence dramatically impairs HSC maintenance and function. For example, deletion of *Huwe1*, a ubiquitin ligase, leads to increased proliferation and stem cell exhaustion via upregulation of N-myc expression.[37] Conditional deletion of *SCF*^{Fbxw7}, another ubiquitin E3 ligase, causes loss of HSC quiescence and stem cell exhaustion via enhancement of c-Myc.[3] In the present study, we found that the E3 ligase TRIM31 could regulate HSC homeostasis and function. *TRIM31* deletion caused enhanced proliferation of LT-HSC and further led to their exhaustion. Furthermore, HSC function was significantly impaired in *TRIM31*$^{-/-}$ mice. In a serial competitive transplantation assay and 5-FU challenge, *TRIM31*$^{-/-}$ HSC showed dramatically reduced self-renewal capacity. TRIM31 was reported to be an E3 ligase in the immune system[11,12] and was also found to play a role in cancer cells.[38,39] Here, we discovered a novel role for TRIM31, which is crucial for the hematopoietic system. Prospectively, TRIM31 could be targeted to regulate HSC maintenance and function.

In human AML, *MLL* is mutated by translocation in about 4% of cases and *MLL* fusion partners include *AF9, ENL*, and *AF4*.[30] Sustaining proliferative signaling is a hallmark of cancer development; and deletion of *TRIM31* promotes breast cancer progression through ubiquitination of p53.[40] Based on our findings of cell proliferation induced by *TRIM31* deletion, we explored the function of TRIM31 in the initiation of AML. TRIM31 may promote leukemia progression through Wnt/β-catenin signaling in AML cell lines.[41] However, by using a murine model of MLL-AF9 in leukemia initiation and development, we demonstrated that *TRIM31* depletion increased the proportion of leukemia-initiating cells and accelerated the kinetics of leukemia development. These effects might be due to the functional mechanisms of TRIM31 varying at different disease stages. Consistent with our results, a database analysis in AML patients also showed that higher expression of TRIM31 correlated with significantly better survival. These data indicate that TRIM31 functions as a suppressor in AML initiation and devel-

opment. Consolidating all the results of the *TRIM31*$^{-/-}$ HSC analysis, TRIM31-mediated control of HSC proliferation is integral to suppress the vulnerability of HSC to leukemic transformation and disease initiation in AML.

Members of the CDK8 module are vital in various cancers and developmental diseases.[42,43] Loss of the CDK8 module member MED12 causes rapid bone marrow failure and acute lethality, showing that MED12 is essential for HSC homeostasis.[44] The kinase activity of CDK8 was reported to be inhibited by small molecules;[45] however, the mechanism of its upstream regulation remains unknown. In this study, we found that CDK8 was regulated by the E3 ligase TRIM31 through ubiquitin-mediated protein degradation. Upregulation of CDK8 in *TRIM31*$^{-/-}$ hematopoietic and

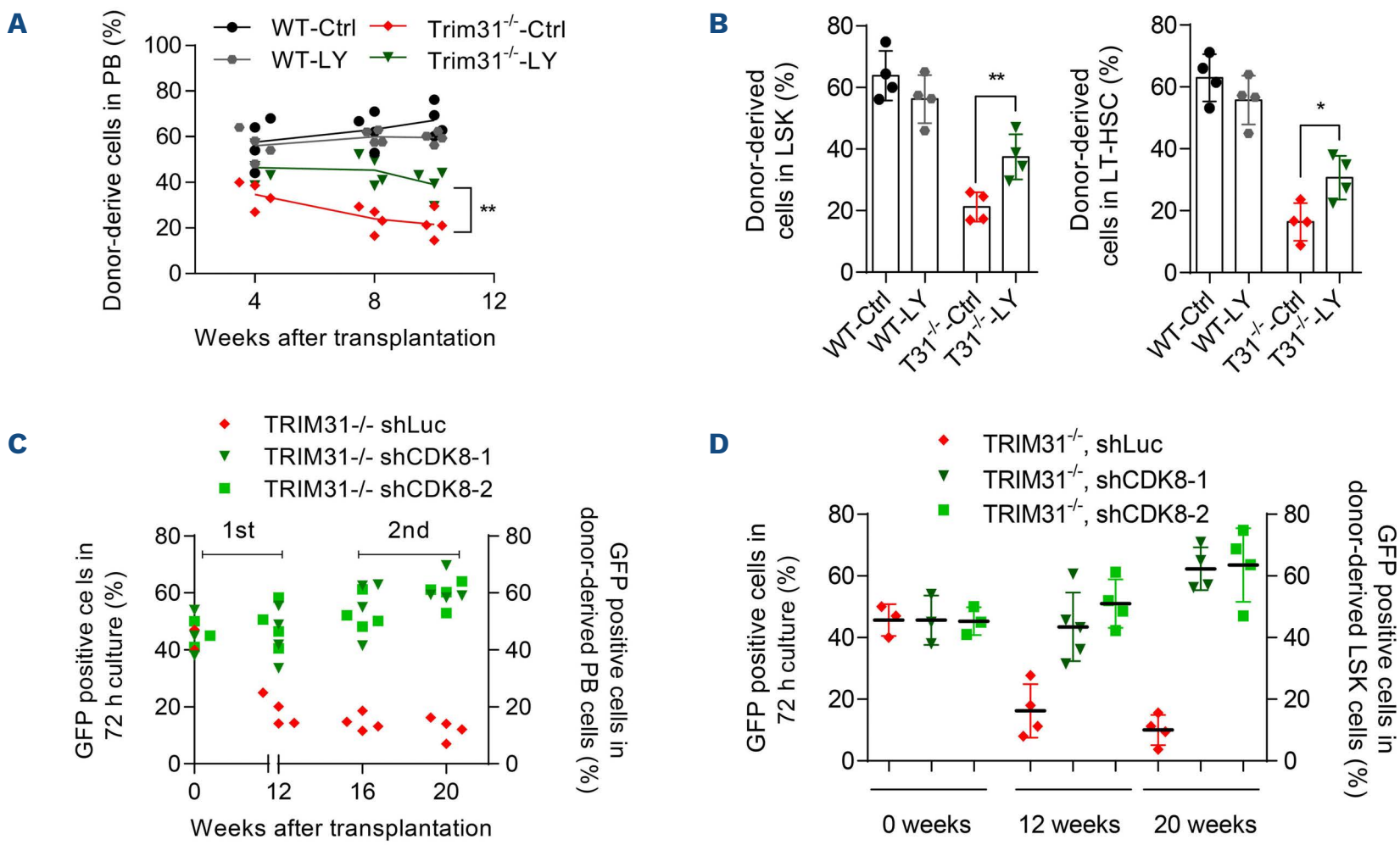

Figure 6. Inhibition and knockdown of CDK8 rescues *TRIM31*$^{-/-}$ hematopoietic stem cell function. (A) Percentage of donor-derived peripheral blood (PB) cells at the indicated time-points after competitive transplantation in long-term hematopoietic stem cells (LT-HSC: CD48^{-}CD150^{+}Flt3^{-} LSK) sorted from wildtype (WT) and *TRIM31*$^{-/-}$ mice treated with a CDK8 inhibitor (LY2857785) (n=4 per group). (B) Percentage of donor-derived LSK (Lin^{-}Sca-1^{+}c-Kit^{+}) cells and LT-HSC 10 weeks after LT-HSC competitive transplantation. (C) The percentage of GFP^{+} cells among donor-derived PB cells after transplantation with shCDK8-1 and -2 virus-infected *TRIM31*$^{-/-}$ LT-HSC (n=4 per group). (D) The percentage of GFP^{+} cells in donor-derived LSK cells after transplantation with shCDK8-1 and -2 virus infected *TRIM31*$^{-/-}$ LT-HSC (n=4 per group). (E) The percentage of G_0 phase (Ki67-negative) cells from mice 12 weeks after transplantation with WT and *TRIM31*$^{-/-}$ LT-HSC infected with shCDK8-1 lentivirus (n=4-5 per group). (F) The knockdown efficiency of shCDK8-1 in GFP^{+} LSK cells after transplantation with shCDK8-1 virus-infected *TRIM31*$^{-/-}$ LT-HSC (n=5-6 mixed per group). All results are presented as the mean ± standard deviation. **P*<0.05; ***P*<0.01; ****P*<0.001. Eight- to 12-week-old WT and *TRIM31*$^{-/-}$ mice were used in the experiment.

leukemia cells leads to enhanced stem cell proliferation, indicating that CDK8 may function as a regulator of cell cycle-related pathways in the hematopoietic system. Therefore, *TRIM31* might be used as a pharmaceutical target in CDK8-enhanced tumors.

CDK8 is reported to be involved in several signaling pathways. In colon cancer, β-catenin hyperactivity promotes cell proliferation and drives tumor transformation which is inhibited by repression of *CDK8* expression.[24] Through the downstream target Myc, CDK8 functions in regulating the pluripotent state of embryonic stem cells.[46] Here, in hematopoietic cells, we found that PBX1 acts as a direct down-

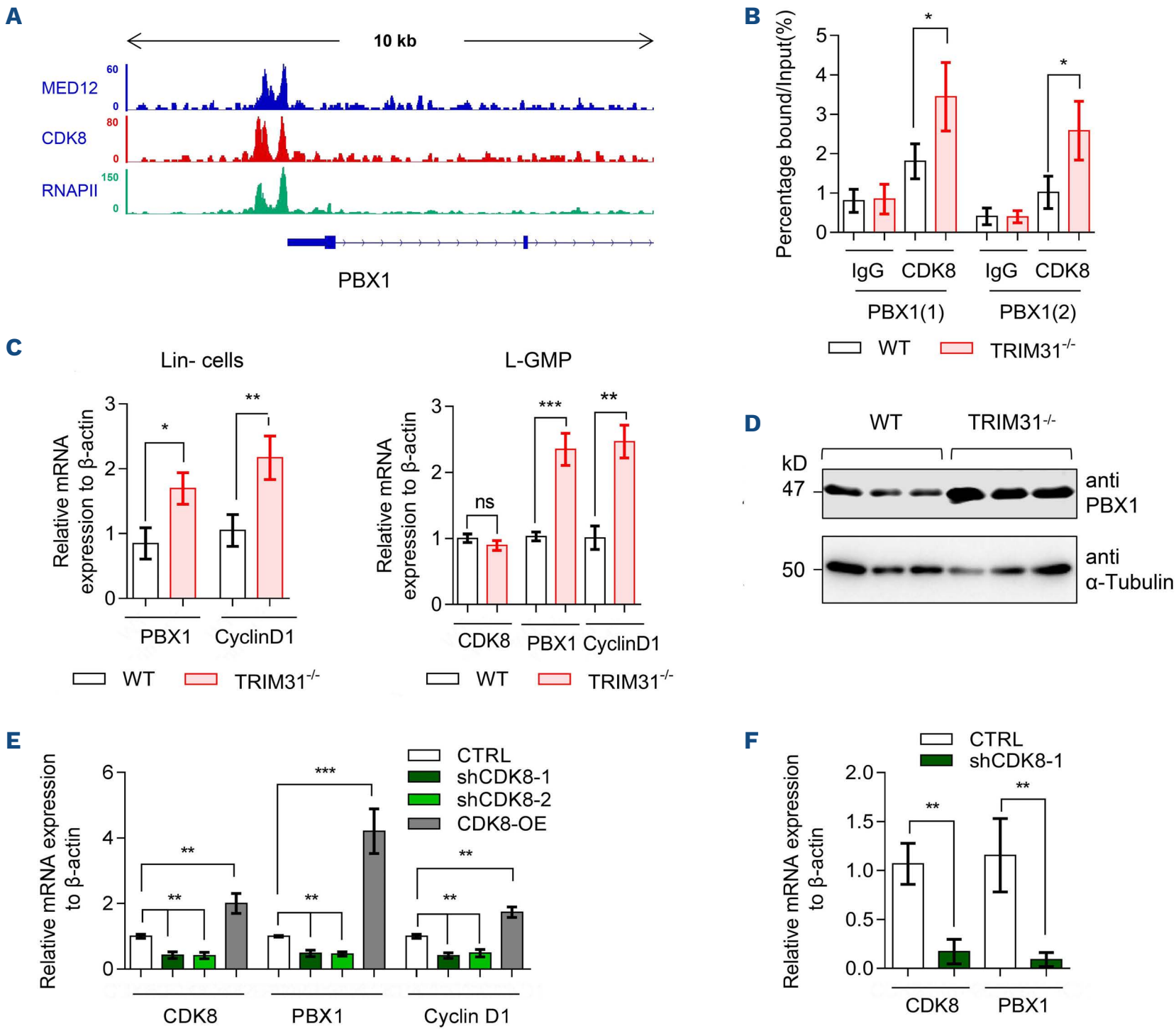

Figure 7. CDK8 regulates the expression of *PBX1* and *cyclin D1*. (A) The binding sites of CDK8, MED12 and RNAPII in the region of the *PBX1* gene are shown. Raw data (from GEO dataset: GSE128242) were analyzed. (B) Real-time polymerase chain reaction (PCR) analysis of CDK8 chromatin immunoprecipitated DNA. Two pairs of primers were designed based on the *PBX1* promoter region (2,000 bp upstream of the start point). For each primer pair, amplifications of chromatin before immunoprecipitation and chromatin immunoprecipitated with preimmune serum were performed as input and negative controls, respectively. The value of bound DNA relative to input is shown as a percentage (n=3 per group). (C) The mRNA levels of *PBX1* and *cyclin D1* in LSK ($Lin^-Sca\text{-}1^+c\text{-}Kit^+$) cells from WT and *TRIM31*$^{-/-}$ mice were measured via real-time PCR. The relative expression was normalized to β-*actin* expression for statistical analysis (n=3 per group). The mRNA levels of *CDK8*, *PBX1* and *cyclin D1* in L-GMP cells from recipient mice transplanted with MLL-AF9 WT and *TRIM31*$^{-/-}$ cells were measured via real-time PCR. The relative expression was normalized to β-*actin* expression for statistical analysis (n=3 per group). (D) Immunoblot of PBX1 in the whole cell lysate of Lin^- cells from WT and *TRIM31*$^{-/-}$ mice. β-actin was used as a loading control (n=3 per group). (E) The relative mRNA expression of *CDK8, PBX1* and *cyclin D1* in 3T3NIH cells with and without *CDK8* knockdown (CDK8-shRNA1, CDK8-shRNA 2) or overexpression (CDK8-OE) was measured via real-time PCR. The relative expression was normalized to β-*actin* expression for statistical analysis (n=3 per group). (F) The relative mRNA expression of *CDK8* and *PBX1* in control and *CDK8* knockdown (GFP^+) Lin^- cells *in vivo*, which were isolated from mice 8 weeks after transplantation with *TRIM31*$^{-/-}$ long-term hematopoietic stem cells (LT-HSC: $CD48^-CD150^+Flt3^-$ LSK) infected with lentivirus. The relative expression was normalized to β-*actin* expression for statistical analysis (n=3 per group). All results are presented as the mean ± standard deviation. **P*<0.05; ***P*<0.01; ****P*<0.001; ns=not significant. Eight- to 12-week-old WT and *TRIM31*$^{-/-}$ mice were used in the experiments.

stream target of CDK8, which binds to the promoter region of *PBX1*; the mRNA expression levels of *PBX1* and *cyclin D1* were upregulated in *TRIM31*$^{-/-}$ mice. CDK8 regulates transcription factors through phosphorylation and proteasomal degradation, suggesting that CDK8 may function as a general regulator of transcription factors.[47] CDK8 acts as a key mediator of BCR-ABL1-driven leukemia through transcriptional changes of the mTOR signaling pathway.[48] In this study, we found that CDK8 regulates cyclin D1 through the transcription factor PBX1. Meanwhile, the association of CDK8 with mediators is reversible and can dramatically alter the structure and function of the mediators.[49] In our context, the accumulation of CDK8 in *TRIM31*$^{-/-}$ hematopoietic and leukemia cells may open the structure of the transcriptional complex and lead to modification of chromosome elements such as histones, further promoting transcription of downstream genes.

PBX1, a proto-oncogene in childhood leukemia, is a typical homeodomain transcription factor belonging to the TALE family. PBX1 is very importantor the hematopoietic system and its downstream targets could be TGFβ and JAK2/Stat3.[35,36] In *TRIM31*$^{-/-}$ mice, cyclin D1 upregulation was induced by enhanced expression of *PBX1* (*Online Supplementary Figure S11G*), which may occur through the Jak2/Stat3 pathway.[36] In addition, cyclin D1 may function together with CDK8 in the hematopoietic system of *TRIM31*$^{-/-}$ mice, although the underlying mechanism needs to be further investigated. In conclusion, the accumulation of CDK8 caused by *TRIM31* deletion induces transcription of *PBX1*, which further leads to upregulation of *cyclin D1* (*Online Supplementary Figure S11H*). Enhancement of CDK8 and PBX1 target genes is observed in human leukemia;[50] therefore, using *TRIM31* as an anti-leukemia target is promising.

Disclosures

No conflicts of interest to disclose.

Contributions

DD and ZJ conceived and designed the experiments. KZ, DL, YL and ZS performed the experiments. KZ and DL analyzed the data. DD, KZ, DL and YL wrote the paper. CG provided TRIM31$^{-/-}$ *mice and JG and HW provided valuable suggestions.*

Acknowledgments

We thank Dr. H. Cheng for his kind gift of the MSCV-MLL-AF9-IRES-GFP encoding plasmid.

Funding

This work was supported by the National Natural Science Foundation of China (grants #81970096 and 91849128 to DD) and the Natural Science Foundation of Guangdong Province, China (#2020A1515010453 to DD); the National Natural Science Foundation of China (#92049304, 82030039), the National Key R&D Program of China (2021YFA1100103) and the Program for Guangdong Introducing Innovative and Entrepreneurial Teams (2017ZT07S347) to ZJ.

Data-sharing statement

All plasmids and cell lines generated in this study are available from the authors upon request.

References

1. Wilson A, Trumpp A. Bone-marrow haematopoietic-stem-cell niches. Nat Rev Immunol. 2006;6(5):93-106.
2. Li J. Quiescence regulators for hematopoietic stem cell. Exp Hematol. 2011;39(5):511-520.
3. Thompson BJ, Jankovic V, Gao J, et al. Control of hematopoietic stem cell quiescence by the E3 ubiquitin ligase Fbw7. J Exp Med. 2008; 205(6):1395-1408.
4. Rathinam C, Matesic LE, Flavell RA. The E3 ligase Itch is a negative regulator of the homeostasis and function of hematopoietic stem cells. Nat Immunol. 2011;12(5):399-407.
5. Rathinam C, Thien CB, Flavell RA, et al. Myeloid leukemia development in c-Cbl RING finger mutant mice is dependent on FLT3 signaling. Cancer Cell. 2010;18(4):341-352.
6. Bai X, Kim J, Yang Z, et al. TIF1gamma controls erythroid cell fate by regulating transcription elongation. Cell. 2010;142(1):133-143.
7. Ito K, Bernardi R, Morotti A, et al. PML targeting eradicates quiescent leukaemia-initiating cells. Nature. 2008;453(7198):1072-1078.
8. Gatt ME, Takada K, Mani M, et al. TRIM13 (RFP2) downregulation decreases tumour cell growth in multiple myeloma through inhibition of NF kappa B pathway and proteasome activity. Br J Haematol. 2013;162(2):210-220.
9. Gandini D, De Angeli C, Aguiari G, et al. Preferential expression of the transcription coactivator HTIF1alpha gene in acute myeloid leukemia and MDS-related AML. Leukemia. 2002;16(2):886-893.
10. Ra EA, Lee TA, Won Kim S, et al. TRIM31 promotes Atg5/Atg7-independent autophagy in intestinal cells. Nat Commun. 2016;24(7):ncomms11726.
11. Song H, Liu B, Huai W, et al. The E3 ubiquitin ligase TRIM31 attenuates NLRP3 inflammasome activation by promoting proteasomal degradation of NLRP3. Nat Commun. 2016;8(7):ncomms13727.
12. Liu B, Zhang M, Chu H, et al. The ubiquitin E3 ligase TRIM31 promotes aggregation and activation of the signaling adaptor MAVS through Lys63-linked polyubiquitination. Nat Immunol. 2017;18(2):214-224.
13. Wang X, Zhang H, Shao Z, et al. TRIM31 facilitates K27-linked polyubiquitination of SYK to regulate antifungal immunity. Signal Transduct Target Ther. 2021;6(1):298.
14. Zeng S, Zhao Z, Zheng S, et al. The E3 ubiquitin ligase TRIM31 is involved in cerebral ischemic injury by promoting degradation of TIGAR. Redox Biol. 2021;45:102058.
15. Zhang J, Cao L, Wang X, et al. The E3 ubiquitin ligase TRIM31

plays a critical role in hypertensive nephropathy by promoting proteasomal degradation of MAP3K7 in the TGF-β1 signaling pathway. Cell Death Differ. 2022;29(3):556-567.
16. Xu M, Tan J, Dong W, et al. The E3 ubiquitin-protein ligase Trim31 alleviates non-alcoholic fatty liver disease by targeting Rhbdf2 in mouse hepatocytes. Nat Commun. 2022;13(1):1052.
17. Marschalek R. Mechanisms of leukemogenesis by MLL fusion proteins. Br J Haematol. 2011;152(2):141-154.
18. Smith LL, Yeung J, Zeisig BB, et al. Functional crosstalk between Bmi1 and MLL/Hoxa9 axis in establishment of normal hematopoietic and leukemic stem cells. Cell Stem Cell. 2011;8(6):649-662.
19. Nguyen AT, Taranova O, He J, et al. DOT1L, the H3K79 methyltransferase, is required for MLL-AF9-mediated leukemogenesis. Blood. 2011;117(25):6912-6922.
20. Taatjes DJ. The human mediator complex: a versatile, genome-wide regulator of transcription. Trends Biochem Sci. 2010;35(6):315-322.
21. Galbraith MD, Allen MA, Bensard CL, et al. HIF1A employs CDK8-mediator to stimulate RNAPII elongation in response to hypoxia. Cell. 2013;153(6):1327-1339.
22. Lai F, Orom UA, Cesaroni M, et al. Activating RNAs associate with Mediator to enhance chromatin architecture and transcription. Nature. 2013;494(7438):497-501.
23. Johannessen L, Sundberg TB, O'Connell DJ, et al. Small-molecule studies identify CDK8 as a regulator of IL-10 in myeloid cells. Nat Chem Biol. 2017;13(10):1102-1108.
24. Firestein R, Bass AJ, Kim SY, et al. CDK8 is a colorectal cancer oncogene that regulates beta-catenin activity. Nature. 2008;455(7212):547-551.
25. Starr TK, Allaei R, Silverstein KA, et al. A transposon-based genetic screen in mice identifies genes altered in colorectal cancer. Science. 2009;323(5922):1747-1750.
26. Kapoor A, Goldberg MS, Cumberland LK, et al. The histone variant macroH2A suppresses melanoma progression through regulation of CDK8. Nature. 2010;468(7327):1105-1109.
27. Pelish HE, Liau BB, Nitulescu II, et al. Mediator kinase inhibition further activates super-enhancer-associated genes in AML. Nature. 2015;526(7572):273-276
28. Hatakeyama S. TRIM proteins and cancer. Nat Rev Cancer Cell. 2011;11(11):792-804.
29. Cheng T, Rodrigues N, Shen H, et al. Hematopoietic stem cell quiescence maintained by p21cip1/waf1. Science. 2000;287(5459):1804-1808.
30. Krivtsov AV, Twomey D, Feng Z, et al. Transformation from committed progenitor to leukaemia stem cell initiated by MLL-AF9. Nature. 2006;442(17):818-822.
31. Huang D, Sun G, Hao X, et al. ANGPTL2-containing small extracellular vesicles from vascular endothelial cells accelerate leukemia progression. J Clin Invest. 2021;131(1):e138986.
32. Yin T, Lallena MJ, Kreklau EL, et al. A novel CDK9 inhibitor shows potent antitumor efficacy in preclinical hematologic tumor models. Mol Cancer Ther. 2014;13(6):1442-1456.
33. Tsai K, Tomomori-Sato C, Sato S, Conaway RC, Conaway J, Asturias F. Subunit architecture and functional modular rearrangements of the transcriptional mediator complex. Cell. 2014;158(2):1430-1444.
34. Moyo MB, Parker JB, Chakravarti D. Altered chromatin landscape and enhancer engagement underlie transcriptional dysregulation in MED12 mutant uterine leiomyomas. Nat Commun. 2020;11(1):1019.
35. Ficara F, Murphy MJ, Lin M, et al. Pbx1 regulates self-renewal of long-term hematopoietic stem cells by maintaining their quiescence. Cell Stem Cell. 2008;2(5):484-496.
36. Wei X, Yu L, Yi L. PBX1 promotes the cell proliferation via JAK2/STAT3 signaling in clear cell renal carcinoma. Biochem Biophys Res Commun. 2018;500(3):650-657.
37. King B, Boccalatte F, Moran-Crusio K, et al. The ubiquitin ligase Huwe1 regulates the maintenance and lymphoid commitment of hematopoietic stem cells. Nat Immunol. 2016;17(11):1312-1321.
38. Sugiura T, Miyamoto K. Characterization of TRIM31, upregulated in gastric adenocarcinoma, as a novel RBCC protein. J Cell Biochem. 2008;105(4):1081-1091.
39. Yu C, Chen S, Guo Y, et al. Oncogenic TRIM31 confers gemcitabine resistance in pancreatic cancer via activating the NF-κB signaling pathway. Theranostics. 2018;8(12):3224-3236.
40. Hanahan D, Robert AW. Hallmarks of cancer: the next generation. Cell. 2011;144(5):646-674.
41. Xiao Y, Deng T, Ming X, Xu J. TRIM31 promotes acute myeloid leukemia progression and sensitivity to daunorubicin through the Wnt/β-catenin signaling. Biosci Rep. 2020;40(4):BSR20194334.
42. Barbieri CE, Baca SC, Lawrence MS, et al. Exome sequencing identifies recurrent SPOP, FOXA1 and MED12 mutations in prostate cancer. Nat Genet. 2012;44(6):685-689.
43. Mäkinen N, Mehine M, Tolvanen J, et al. MED12, the mediator complex subunit 12 gene, is mutated at high frequency in uterine leiomyomas. Science. 2011;334(6053):252-255.
44. Aranda-Orgilles B, Saldaña-Meyer R, Wang E, et al. MED12 regulates HSC-specific enhancers independently of mediator kinase activity to control hematopoiesis. Cell Stem Cell. 2016;19(6):784-799.
45. Dale T, Clarke PA, Esdar C, et al. A selective chemical probe for exploring the role of CDK8 and CDK19 in human disease. Nat Chem Biol. 2015;11(12):973-980.
46. Adler AS, McCleland ML, Truong T, et al. CDK8 maintains tumor dedifferentiation and embryonic stem cell pluripotency. Cancer Res. 2012;72(8):2129-2139.
47. Alarcón C, Zaromytidou AI, Xi Q, et al. Nuclear CDKs drive Smad transcriptional activation and turnover in BMP and TGF-β pathways. Cell. 2009;139(4):757-769.
48. Menzl I, Zhang T, Berger-Becvar A, et al. A kinase-independent role for CDK8 in BCR-ABL1+ leukemia. Nat Commun. 2019;10(1):4741.
49. Tsai KL, Sato S, Tomomori-Sato C, et al. A conserved Mediator-CDK8 kinase module association regulates Mediator-RNA polymerase II interaction. Nature Struct Mol Biol. 2013;20(5):611-619.
50. Alsadeq A, Schewe DM. Acute lymphoblastic leukemia of the central nervous system: on the role of PBX1. Haematologica. 2017;102(4):611-613.